Boletim da Sociedade Astronômica Brasileira, **35**, no. 1, 228-231

Alfvén waves propagation in differentially rotating astrophysical disks

N. F. S. Andrade & V. Jatenco-Pereira

[1] Instituto de Astronomia, Geofísica e Ciências Atmosféricas – USP; e-mail: natalia.fernanda.andrade@usp.br

Abstract. The transport of angular momentum and matter are vital mechanisms in understanding the evolution of astrophysical disks, particularly protostellar disks. In recent years, the role of non-ideal MHD effects in those objects has been widely explored, and it is now known that those effects significantly impact the viability of the Magneto-Rotational Instability (MRI) and the transport of angular momentum in general. Those terms tend to suppress the development of the MRI. On the other hand, we have previously studied, using a local approximation, where the radial shear is written as $\mathbf{v} = -q\Omega_0 x\hat{\mathbf{y}}$, the damping of surface Alfvén waves for Keplerian disks ($q = 3/2$) as a possible source of disk heating. We generalize this model by considering a rotating disk with an angular velocity given by r^{-q} for any given value of q, thus ensuring a more global profile for the radial shear. For objects subject to viscosity, we have found that the radial shear associated with the differential rotation can either increase the damping rate or amplify the wave's amplitude (i.e., trigger an instability), depending on its propagation properties. More importantly, our current results indicate that the overall behavior of the damping rate/growth rate is generally independent of the value of q for the work hypotheses adopted. Now, since the non-ideal MHD terms directly impact the magnetic flux of the plasma, they will also influence the propagation of MHD waves. Thus, the dissipative MHD effects are also good candidates to promote the Alfvén waves damping. Therefore, in this work, we also investigated the consequences of the non-ideal MHD effects on wave damping and obtained, as expected, that the amount of heating in the dissipative layer is independent of the resistivity coefficient, which guarantees that the damping rate/instability growth rate that we obtained remains valid for resistive MHD. In this scenario, we may expand the regions where the MRI is active due to the increase in the ionization fraction associated with these environments heating.

Resumo. O transporte de momento angular e matéria são processos fundamentais para a evolução de discos astrofísicos, particularmente discos protoestelares. Nos últimos anos, o papel dos efeitos MHD não-ideais nestes objetos tem recebido bastante atenção e sabe-se que a presença destes efeitos impactam a viabilidade da Instabilitade Magneto-Rotacional (MRI, do inglês *Magneto-Rotational Instability*), e o transporte de momento angular em geral. Estes termos tendem a suprimir o desenvolvimento da MRI. Por outro lado, nós já investigamos, através de um aproximação local, onde o *shear* radial é escrito como $\mathbf{v} = -q\Omega_0 x\hat{\mathbf{y}}$, o amortecimento de ondas Alfvén de superfície para discos Keplerianos ($q = 3/2$) como uma possível fonte de aquecimento do disco. Agora, nós generalizamos esse modelo para discos com velocidades angular descritas por r^{-q} para valores quaisquer de q, assegurando, assim, um perfil mais global para o *shear* radial. Para objetos sujeitos à viscosidade, nós obtivemos que o *shear* radial associado com a rotação diferencial pode ou aumentar a taxa de amortecimento ou aumentar a amplitude da onda (i.e., originar uma instabilidade), dependendo das propriedades de propagação. Especialmente, nossos resultados atuais indicam que o comportamento geral da taxa de amortecimento/crescimento é, de maneira geral, independente do valor de q para as hipóteses de trabalho adotadas. Agora, como os efeitos MHD não-ideais impactam diretamente sobre o fluxo magnético d plasma, eles também irão influenciar a propagação de ondas MHD. Logo, os efeitos MHD dissipativos são também bons candidatos para promover o amortecimento de ondas Alfvén. Portanto, neste trabalho, nós também investigamos as consequências dos efeitos MHD não-ideais no amortecimento das ondas e encontramos, como esperado, que o total de amortecimento na camada dissipativa é independente do coeficiente de resistividade, o que garante que a taxa de amortecimento/taxa de crescimento da instabilidade que obtivemos permanece válido para o MHD resistivo. Neste cenário, é possível expandir as regiões onde a MRI é ativa devido ao aumento da fração de ionização associado ao aquecimento destes ambientes.

Keywords. Accretion, accretion disks – Magnetohydrodynamics (MHD)

1. Introduction

The evolution of astrophysical disks is intrinsically associated with the transport of angular momentum (AM) and matter in these environments. However, despite its great importance, the process behind the angular momentum transfer is still poorly understood. Throughout the years, a number of mechanisms have been proposed to explain this phenomenon, such as the Magneto-Rotational Instability (MRI, Balbus & Hawley 1991). This instability, however, may not be efficient in partially ionized plasmas (e.g. Lesur et al. 2014), where non-ideal MHD effects become important. Thus, in some portions of the disks, where MRI is ineffective, the accretion process does not take place due to the lack of AM transport. At the same time, those disks may be populated by MHD waves, since they are magnetized. Vasconcelos et al. (2000) proposed that, in those regions where MRI is quenched, or its efficienty is highly reduced, the damping of Alfvén waves could act as a heating source, increasing the ionization fraction of the disks, 'reviving' the MRI. In this work, we use this same hypothesis and investigate how the resonant absorption of Alfvén waves, in the presence of a radial shear associated with the differential rotation, impact on these wave properties. This manuscript is organized as follows: in Section 2 we briefly introduce the disk model and hypotheses adopted; in Section 3 we show some representative results for a particular example and, finally, in Section 4, we draw the main conclusions and discuss some necessary improvements to the model.

2. The model

The dynamics of accretion disks is described the MHD equations. If we postulate that the effects of resonance are localized, we may describe the fluid properties with a local approximation. In this scenario, we restrict our analysis to the vicinity of our reference point, r_0, in the sense that a new local cartesian system of coordinates, centered at r_0 is defined, and the background velocity, associated with the radial shear due to the differential

rotation, is given by (Lesur 2021):

$$v_0 = -q\Omega_0 x\hat{\mathbf{y}}. \tag{1}$$

It is possible to simplify our equations even more if we explore the fact that only Alfvén waves are under consideration in the present work. Thus, the continuity equation reduces to the incompressibility condition (Equation 2a), whereas the viscosity and resistivity are considered in the equations of motion and induction (Equation 2b and 2c, respectively).

$$\boldsymbol{\nabla}.\boldsymbol{v} = 0 \tag{2a}$$

$$\partial_t \boldsymbol{v} + \boldsymbol{v}.\boldsymbol{\nabla}\boldsymbol{v} = -\frac{1}{\rho}\boldsymbol{\nabla} p + \frac{(\boldsymbol{\nabla}\times\boldsymbol{B})\times\boldsymbol{B}}{4\pi\rho} - 2\Omega_0\hat{\mathbf{z}}\times\boldsymbol{v} + 3x\Omega_0^2\hat{\boldsymbol{x}} + \nu\nabla^2\boldsymbol{v} \tag{2b}$$

$$\partial_t \boldsymbol{B} = \boldsymbol{\nabla}\times\big[\boldsymbol{v}\times\boldsymbol{B} - \eta\boldsymbol{\nabla}\times\boldsymbol{B}\big]. \tag{2c}$$

In the above equations, ν and η correspond to the kinematic viscosity and resistivity, respectively, and both quantities are taken as constants. Also, Ω_0 denotes the angular velocity of the fluid, evaluated at r_0. All of the other variables have their usual definitions. If we assume that, in the equilibrium, the background velocity is given by Equation 1, at the same time that $p_0 = p_0(x)$, $\boldsymbol{B_0} = B_0(x)\hat{\mathbf{z}}$, while the gas density remains somewhat unchanged ($\rho_0 \sim$ cte), we find that the following relation is satisfied:

$$\frac{1}{\rho_0}\Big[\partial_x p_0 + \frac{B_0\partial_x B_0}{4\pi}\Big] = -(2q-3)\Omega_0^2 x. \tag{3}$$

If we now apply disturbances to our system of the form:

$$g(x,y,z,t) = g(x)\exp[i(-\omega t + k_z z + k_y y)], \tag{4}$$

where ω is the frequency of the perturbation, k_y, and k_z are the 'azimuthal' and 'vertical' wavenumbers, respectively, and the amplitude of the perturbation is a function of x, and assume that the gas pressure and magnetic and velocity fields exhibit perturbations given by $p = p_0 + p_1$, $\boldsymbol{B} = (\boldsymbol{B_{1x}}, \boldsymbol{B_{1y}}, \boldsymbol{B_0} + \boldsymbol{B_{1z}})$, $\boldsymbol{v} = (\boldsymbol{v_{1x}}, \boldsymbol{v_0} + \boldsymbol{v_{1y}}, 0)$, we acquire 2 ODEs responsible for describing the medium:

$$\overline{\omega}_\eta^2\Big[\frac{\overline{\omega}_\eta^2\overline{\omega}_\nu^2}{\overline{\omega}^2} - \omega_A^2\Big](\partial_x\xi_x) = -2\overline{\omega}k_y\Omega_0\xi_x\Big[q\Big\{\frac{\overline{\omega}_\eta^2}{\overline{\omega}}\Big(\frac{\overline{\omega}_\eta^2\overline{\omega}_\nu^2}{\overline{\omega}^2} - \omega_A^2\Big)\overline{\omega}\Big(\frac{\overline{\omega}_\eta^4}{\overline{\omega}^2} - \omega_A^2\Big)\Big\} + 2\frac{\overline{\omega}_\eta^4}{\overline{\omega}}\Big] + k_y^2\frac{p_T}{\rho_0} \tag{5a}$$

$$\overline{\omega}_\eta^2\Big[\frac{\overline{\omega}_\eta^2\overline{\omega}_\nu^2}{\overline{\omega}^2} - \omega_A^2\Big]\frac{\partial_x p_T}{\rho_0} = \xi_x\overline{\omega}^2\Big\{\Big(\frac{\overline{\omega}_\eta^2\overline{\omega}_\nu^2}{\overline{\omega}^2} - \omega_A^2\Big)^2 + 2\Omega_0^2\Big[q\Big(\frac{\overline{\omega}_\eta^4}{\overline{\omega}^2} - \omega_A^2\Big) - 2\frac{\overline{\omega}_\eta^4}{\overline{\omega}^2}\Big]\Big\} + 2k_y\Omega_0\frac{\overline{\omega}_\eta^4}{\overline{\omega}}\frac{p_T}{\rho_0}, \tag{5b}$$

where $\xi_x = iv_{1x}/\overline{\omega}$ is the Lagrangian 'radial' displacement, $p_T = p_1 + B_0B_{1z}/4\pi$ corresponds to the total pressure perturbation, $\overline{\omega} = \omega + k_y q\Omega_0 x$ is the Doppler-shifted frequency, $\omega_A^2 = k_z^2 v_A^2$ denotes the Alfvénic frequency and $\overline{\omega}_{\nu,\eta}^2 = \overline{\omega}^2 - i(\nu,\eta)\nabla^2\overline{\omega}$.

Now, if we assume that dissipative effects are important only near the resonance point, x_A, defined by $\overline{\omega}^2(x_A) = \omega_A^2(x_A)$ (Erdélyi et al 1995), Equations 5a and 5b yield the new ODE, written as:

$$\frac{d}{dx}\Big[\Big(\frac{\overline{\omega}_\eta^2\overline{\omega}_\nu^2}{\overline{\omega}^2} - \omega_A^2\Big)\partial_x\xi_x\Big] = k_y^2\Big(\frac{\overline{\omega}_\eta^2\overline{\omega}_\nu^2}{\overline{\omega}^2} - \omega_A^2\Big)\xi_x, \tag{6}$$

where we have assumed that the resistive effects are dominant in relation to the viscous one, and aopted $R_{eM} \sim 10^3 - 10^4$.

If we postulate that the interface has a width $2a$, centered at $x = 0$, equation 6 is used to obtain ξ_x in two different regimes: first, we assume that in the regions 'away' from the interface, i,e. $|x| \geq a$, the background properties can be approximated as constants, which entails the following solution for the above equation:

$$\begin{aligned}\xi_x(x) &= c_1\exp(k(x+a)),\ \ x \leq -a\\ \xi_x(x) &= c_2\exp(-k(x-a)),\ \ x \geq a,\end{aligned} \tag{7}$$

where c_1 and c_2 are constants. For the region within this interface of width $2a$, on the other hand, we retain the x dependence of the equilibrium properties and, under the hypothesis $k_y a \ll 1$, we find that within this interface ξ_x is given by:

$$\xi_x(x) = \xi_{x_0} + \int_{-a}^{x}\frac{c'}{(\overline{\omega}_\eta^2\overline{\omega}_\nu^2/\overline{\omega}^2 - \omega_A^2)}dx, \quad |x| \leq a, \tag{8}$$

where ξ_{x_0} is evaluated at $x = -a$. Now, due to our initial conditions, the relevant quantity for our analysis is the Lagrangian pressure perturbation, defined in Equation 9:

$$\Delta\frac{p_T}{\rho_0} = \frac{p_T}{\rho_0} - (2q-3)\Omega_0^2 x, \tag{9}$$

which is constant across the interface of width $2a$ (Hollweg et al 1990). Thus, applying the continuity of both $\Delta p_T/\rho_0$ and ξ_x at $x = \pm a$, we can write the dispersion relation $D(\omega, x)$, using the perturbation method, as:

$$D(\omega,x) \sim D_0(\omega) + D_1(\omega,x); \tag{10a}$$

$$D_0(\omega) = c_2\exp(-ka)k[(\overline{\omega}_-^2 - \omega_{A_-}^2) + (\overline{\omega}_+^2 - \omega_{A_+}^2)], \tag{10b}$$

$$D_1(\omega,x) = c_2\exp(-ka)[-6k_y^2\Omega_0^2 a] - \Big(\int_{-a}^{a}\frac{c'}{(\overline{\omega}^2 - \omega_A^2 - i\overline{\omega}\nu\partial_x^2)}dx\Big)\times \times[-k(\overline{\omega}_+^2 - \omega_{A_+}^2) + k_y\Omega_0(2\omega + 3k_y\Omega_0 a)], \tag{10c}$$

where $D_1/D_0 = O(ka) \ll 1$ e $|v_0| = q\Omega_0 a$. Defining the perturbation frequency as $\omega = \omega_0 + \omega_1$, with $|\omega_0| \gg |\omega_1|$ (e.g. Bahari et al 2020), $D(\omega, x)$ can be written as:

$$D(\omega,x) \sim D_0(\omega_0) + D_1(\omega_0,x) + \omega_1\frac{\partial D_0}{\partial\omega}\Big|_{\omega=\omega_0}, \tag{11}$$

where we performed a Taylor expansion. Now, since $\omega_1 \ll \omega_0$, if we define $\omega_1 = \omega_{1r} - i\gamma$, we find that ω_{1r} provides only small corrections to ω_0. On the other hand, γ gives the damping rate (if $\gamma > 0$) or growth rate of an instability (if $\gamma < 0$). Therefore, since $D(\omega, x) = 0$, if we equate the first and second order equations to zero, we acquire the perturbation frequency, ω_0, and the rate, γ, which is defined as:

$$\gamma = \Big(\tfrac{1}{4\omega_0}\Big)k(\overline{\omega}_-^2 - \omega_{A_-}^2)\Big\{\tfrac{\pi\epsilon}{\Delta}[(\overline{\omega}_-^2 - \omega_{A_-}^2) + \mathrm{sign}(k_y)\Omega_0(2\omega + 3k_y\Omega_0 a)]\Big\}\Big|_{\omega=\omega_0}, \tag{12}$$

where $\Delta = \partial_x(\overline{\omega}^2 - \omega_A^2)\big|_{x=x_A}$ and $\epsilon \equiv \mathrm{sign}(\overline{\omega}_0/\Delta)$. It is important to emphasize that in deriving Equation 12, we considered only the effects associated with the resonance, which allowed us to use the previous result obtained by Sakurai (1991) when evaluating the integral in Equation 10c.

3. Results

Below, we exhibit some representative results of the main features observed. In all cases displayed, we have considered only positive wavenumbers, i.e. $k_y, k_z > 0$, and fixed $k_y a = 10^{-3}$. Also, we assumed that $k_z/k_y = 10$ and defined that the Alfvénic velocity decreases with increasing x, satisfying the following relation $v_{A+}/v_{A-} = 1/\sqrt{3}$, where v_{A+} corresponds to the Alfvén velocity at $x = a$ and v_{A-} denotes this same velocity at $x = -a$, with the profile of ω_A within the region defined by $-a \leq x \leq a$ given by:

$$\omega_A^2(x) = \frac{\omega_{A+}^2 + \omega_{A-}^2}{2} + (\omega_{A+}^2 - \omega_{A-}^2)\frac{x}{2a}. \tag{13}$$

Here, two distint cases were considered: the *forward* case, with frequency defined as ω_0^+, and the backward one, with ω_0^-, where these quantities satisfy: $\omega_0^{\pm}/\omega_{A-} = \pm|\omega_0/\omega_{A-}|$.

In Figures 1 and 2 we show the damping rate ($\gamma/|\omega_0| > 0$) or growth rate ($\gamma/|\omega_0| < 0$), both normalized by ω_0, for the forward and backward cases, respectively, for different values of q, as a function of $\Omega_0 a/v_{A-}$ (bottom x-axis) and the resonance position, $|x_A/a|$ (top x-axis). In Figure 1, the dashed lines represent the growth rate of an instability, whereas the full lines are associated with the damping rate, in both figures. From the analysis of these plots, we find that for all values of q considered, a significant difference is observed for the forward and backward scenarios: while in the first (Figure 1) $\gamma/|\omega_0|$ changes sign in $\Omega_0 a/v_{A-} \sim 2 \times 10^{-3}$, in the latter, this transition is not observed, at least in the range considered. It is natural, then, to conclude that for $\mathrm{sign}(\omega_0/\omega_{A-}) > 0$, an instability is triggered for a critical value of the velocity shear, $\Omega_0 a/v_{A-}$. From Equation 12, we note that two situations could explain this observed transition: the difference between $\overline{\omega}$ and the Alfvénic frequency, evaluated in $x = -a$, must vanish ($\overline{\omega}_-^2 - \omega_{A-}^2 = 0$), indicating that this shift is related to the resonance, or γ must vanish when $\Delta p_T/\rho_0 = 0$. The second option seems to be the correct one, as we will see shortly. The backward waves, on the other hand, are always damped, with a continuous increase in the damping rate with $\Omega_0 a/v_{A-}$. In both cases, however, γ goes to 0 for large values of $\Omega_0 a/v_{A-}$.

As previously stated, the top x-axis displays the ratio between the absolute value for resonance position and a. The position x_A/a is obtained through the equality $\overline{\omega}^2(x_A) = \omega_A^2(x_A)$. Suppose we focus on this axis in Figures 1 and 2 and recall that the resonant damping/instability occurs only for $|x_A A/a| < 1$. In that case, we can infer that the second root for γ for the forward waves (and only root for the backward ones) is directly related to the resonance of the surface Alfvén waves. This confirms our previous claim that the regime shift observed in Figure 1 is associated with the Lagrangian pressure perturbation since our $k_y a \ll 1$ hypothesis entails that the term $\overline{\omega}_-^2 - \omega_{A-}^2$ will remain somewhat unaltered, for the backward and forward scenarios, except for very large values of $\Omega_0 a/v_{A-}$, implying that if the resonance was responsible for the development of the instability observed in Figure 1, the same behaviour should have been observed in Figure 2.

Finally, from the results displayed above, in differentially rotating disks, the rotation itself appears to be the most important effect in the resonance of surface Alfvén waves, at least for our work hypotheses. This can be gathered by the fact that there is no significant variation in the presented curves of $\gamma/|\omega_0|$ for different values of q, indicating that the radial shear may not be as effective in the description of the propagation of surface Alfvén waves, at least in the limits considered in this work.

4. Conclusions

In this work, we investigated the effects of resonant absorption on the properties of Alvén waves that populate astrophysical disks that exhibit differential rotation. The impact of the differential rotation is represented by the parameter q in the definition of the radial shear. We considered two different scenarios: the forward case, where $\mathrm{sign}(\omega_0/\omega_{A-}) > 0$, and the backward case, with $\mathrm{sign}(\omega_0/\omega_{A-}) < 0$. We found that whereas for the forward waves, the waves are initially damped, for small values of $\Omega_0 a/v_{A-}$, and then become subject to an instability for the backward waves, those waves are always damped, presenting damping rates as high as $\gamma/|\omega_0| \sim 10^{-2}$. This feature could indicate that this mechanism can be a good candidate for increasing the disk ionization fraction due to the heating associated with the waves damping.

It is now necessary, however, to discuss some limitations to our model. To provide an analytical description of this phenomenon, we made some simplifying considerations. The results showed above are valid only in the limit $\frac{\eta,\nu\nabla^2}{k_y q \Omega_0 x} \ll 1$, when the effects of these dissipative terms become essential only in the vicinity of the resonance point. Thus, to make this mechanism valid for astrophysical disks in general, we must eliminate this restriction over the values of ν and η.

Acknowledgements. The authors would like to thanks the Brazilian agency FAPESP (under grant 2019/26787-3) for financial support.

References

Bahari, K., Petrukhin, N. S., & Ruderman, M. S. 2020, MNRAS, 496, 67
Balbus, S.A., & Hawley, J.F. 1991, ApJ, 376, 214
Erdélyi R., Goossens, M. & Ruderman, M.S. 1995, Sol. Phys., 161, 123
Hollweg J.V., Yang, G., Cadez V.M. & Gakovic, B. 1990, ApJ, 349, 335
Lesur, G., Kunz, M. W., & Fromang, S. 2014, A&A, 566, A56
Lesur G.R.J. 2021, J. Plasma Phys., 87, 205870101
Sakurai, T., Goossens, M., & Hollweg, J. V. 1991, Sol. Phys., 133, 227
Vasconcelos, M., Jatenco-Pereira, V., & Opher, R. 2000, ApJ, 534, 967

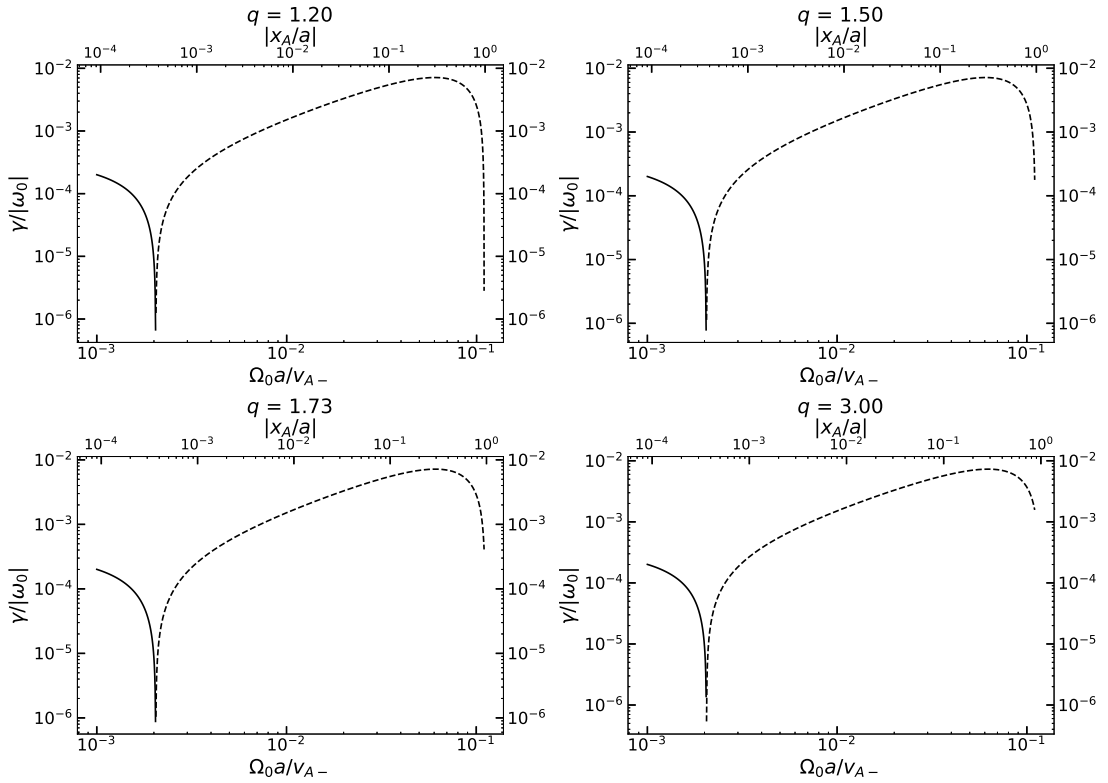

Figure 1. Profile of $\gamma/|\omega_0|$ as a function of $\Omega_0 a/v_{A-}$ (bottom x-axis) and the absolute value of the resonant field line , $|x_A/a|$ (top x-axis), for the forward waves (sign$(\omega_0/\omega_{A-}) > 0$) for different values of q, increasing from the upper left panel ($q = 1.20$) to the bottom right panel ($q = 3$). The solid and dashed lines correspond to the damping rates and the growth rate of an instability, respectively.

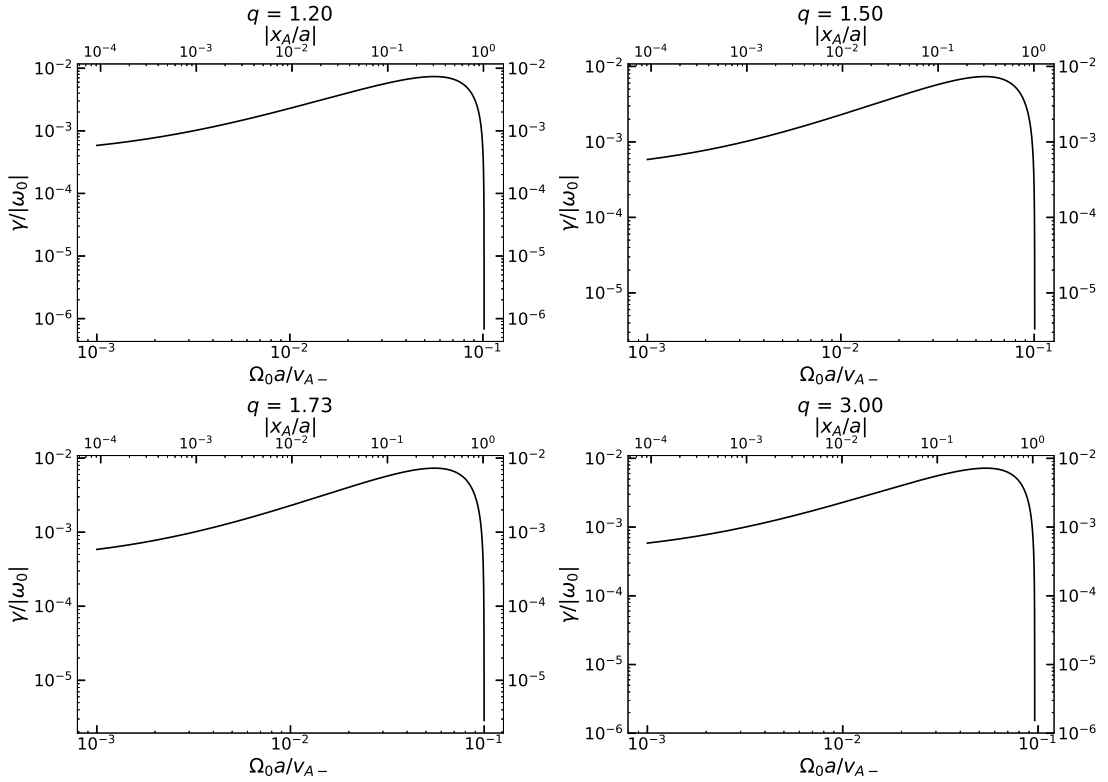

Figure 2. Same as Figure 1, but for the backward waves ($\omega_0/\omega_{A-}) < 0$). Note that now the waves are always damped, at least in the velocity range shown.